

Solubility in the Quaternary $\text{Na}_2\text{O}-\text{V}_2\text{O}_5-\text{CaO}-\text{H}_2\text{O}$ System at (40 and 80) °C

Lanjie Li,^{†,‡} Hao Du,[‡] Na Yang,[‡] Shaona Wang,^{*,‡} Shili Zheng,[‡] and Yi Zhang[‡]

[†]School of Materials & Metallurgy, Northeastern University, Shenyang, Liaoning 110004, People's Republic of China

[‡]National Engineering Laboratory for Hydrometallurgical Cleaner Production Technology, Key Laboratory of Green Process and Engineering, Institute of Process Engineering, Chinese Academy of Sciences, Beijing 100190, People's Republic of China

ABSTRACT: The conversion of $\text{Na}_3\text{VO}_4 \cdot n\text{H}_2\text{O}$ to calcium vanadate is one of the key operation units of the vanadium cleaner production process. The solubility data for the $\text{Na}_2\text{O}-\text{V}_2\text{O}_5-\text{CaO}-\text{H}_2\text{O}$ system at (40 and 80) °C therefore were studied in a wide alkali concentration range from (40 to 540) $\text{g} \cdot \text{L}^{-1}$ Na_2O in order to optimize the conversion process. From the data, a method of producing calcium vanadate from $\text{Na}_3\text{VO}_4 \cdot n\text{H}_2\text{O}$ and leaching calcium vanadate from vanadium slag and other calcium vanadate containing materials is proposed.

INTRODUCTION

Vanadium, due to its outstanding physical and chemical properties,^{1–3} such as high tensile strength, hardness, fatigue resistance, and resistance to oxidization in air, acid, and alkali solutions,^{4–6} is widely used in humidity sensors, electrochromic devices, astronautics industry, and ceramic industry. In addition, vanadium can be used as catalysts,^{7,8} particularly in the manufacture of sulfuric acid. Also, vanadium as an important electrochemical raw material, is widely used in the production of vanadium battery, due to its excellent electrochemical properties, such as complete charge–discharge, fast response time, renewable energy, uninterrupted power supplying, facile transformation of electric capacity.^{9–11} However, the primary use of vanadium is in the iron and steel industry as alloying element. And, the steel mechanical properties such as high tensile strength, hardness, and fatigue resistance will be significantly improved with the addition of vanadium (around 50 $\text{g} \cdot \text{T}^{-1}$ in China, and 80–100 $\text{g} \cdot \text{T}^{-1}$ in Europe). As the fast development of iron and steel industry in China, the requirement for vanadium will be significantly increased in the future.

Vanadium-bearing slag is one of the most important sources of vanadium extration, accounting for 58 % of vanadium production globally.¹² Roasting of vanadium slag with sodium salts is currently the most popular vanadium extraction process,¹³ and the main operating units include roasting, leaching, solution purification, and vanadium precipitation.¹⁴ The sodiation roasting of vanadium slag technology is simple and easy to operate, but this process suffers from the low vanadium extraction efficiency and release of toxic gases such as HCl and Cl_2 , causing serious environmental pollutions.¹⁵ Thus, a highly efficient and environmental friendly vanadium extraction process has been studied by the Institute of Process Engineering, Chinese Academy of Sciences.¹⁶ In the new cleaner process, highly concentrated NaOH solution was introduced to extract vanadium from vanadium slag, and the vanadium compound was converted to water-soluble sodium vanadate after oxidation, achieving nearly 95 % vanadium recovery. As a cleaner

vanadium production process, the new process exhibits a promising prospect for remarkably improving the resources and energy utilization efficiency and achieving minimal tailings production.

In the green process, $\text{Na}_3\text{VO}_4 \cdot n\text{H}_2\text{O}$ was separated from the system by cooling crystallization.⁵ $\text{Na}_3\text{VO}_4 \cdot n\text{H}_2\text{O}$, as the intermediate product in this green process, cannot be used directly in the iron and steel industry and as electrochemical materials directly, due to its high sodium content and low purity (around 90 %). Thus, further treatment of $\text{Na}_3\text{VO}_4 \cdot n\text{H}_2\text{O}$ is needed. Precipitation of vanadate ions using calcium ions appears to be an attractive approach due to the fact that both vanadium and calcium are useful elements in vanadium iron production. $\text{Na}_3\text{VO}_4 \cdot n\text{H}_2\text{O}$ hydrolyzes in water, forming alkaline solutions, and the solution alkalinity increases with the vanadium concentration. Therefore, it is important to study the calcium precipitation conditions, such as the solution concentrations, alkalinity, temperature, and etc. The solubility phase diagram of vanadium compounds in alkaline solution with the presence of calcium oxide is thus of great interest for the understanding of vanadate ion precipitation reaction. Due to the lack of such data in the literature, the solubility phase diagram of vanadate in NaOH solution at (40 and 80) °C were examined and analyzed, respectively, and solid phases formed at different conditions were discussed.

EXPERIMENTAL SECTION

Apparatus and Reagents. A specially designed HZ-9612K thermostatted shaking air bath with a precision of 0.2 °C was used for preparing samples at (40 and 80) °C. Polyethylene bottles, each 200 cm^3 capacity, containing the planed excess of the solid phase and sodium hydroxide solution and solid $\text{Ca}(\text{OH})_2$, were used for shaking and placed in the thermostat.

Received: July 6, 2011

Accepted: September 9, 2011

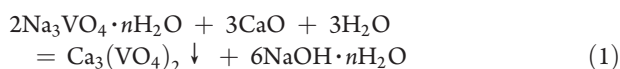
Published: September 28, 2011

The component of the equilibrium alkaline solutions was determined using ICP-OES (PE Optima 5300DV, Perkin-Elmer). The solution density was measured by densimeter of glass floating meter (SY-02, Liaoning Huake oil equipment technology Co., LTD). Crystallographic information of the equilibrium solid-phases were obtained from powder X-ray diffraction analysis (XRD, Philips PW223/30 with Cu K α radiation, 40 kV and 100 mA).

All chemicals used in this work, including NaOH, Na₃VO₄·12H₂O, and Ca(OH)₂, were of analytical grade and manufactured by Sinopharm Chemical Reagent Company. High-purity Milli-Q water, with a resistivity of above 18.2 M Ω ·cm at ambient temperature, was used.

PROCEDURE

In order to determine the compositions of the equilibrium solutions in the eutonic points saturated with Na₃VO₄ and Ca(OH)₂ and to determine the equilibrium solid-phases of the precipitates, the study of the reciprocal solubility of Na₃VO₄ and Ca(OH)₂ in the NaOH solution was performed at (40 and 80) °C.



The saturated solutions were prepared by the following method. The polyethylene bottles, containing 20 g of Na₃VO₄·12H₂O and 5.55 g of Ca(OH)₂ (Ca/V molar ratio at 3/2) in 200 cm³ NaOH solutions (concentration ranging between (50 and 700) g·L⁻¹), were placed in the thermostatted shaking air bath equipment maintained at temperature (80 and 40) °C. These solutions were constantly shaken in the thermostat for a week to achieve the complete dissolution. After a week, the shaking was stopped, and the samples were kept in the baths for two more days for the suspended precipitates to sediment. Next, sampling of the liquid phase and precipitate phase were performed to determine whether the solution was saturated, and the saturated station was supposed to be achieved when the composition of liquid phase did not change with time, and equilibrium solid-phase presented vanadium-bearing phase. If the liquid phase of the sample prepared did not achieve saturation, another 20 g of Na₃VO₄·12H₂O and 5.55 g of Ca(OH)₂ were added into the polyethylene bottles until the vanadium containing phase in the equilibrium solid-phase was observed.

In order to guarantee the accuracy of the solubility data, excessive amounts of Na₃VO₄·12H₂O and Ca(OH)₂ were mixed into NaOH solutions with predetermined concentration, and the suspension was stirred in a flask positioned in a constant temperature electric oven at about 90 °C. After stirring about 12 h, these solutions were then transferred into sealed polyethylene bottles, which were then placed in thermostatted air shaking baths with temperature maintained at (80 and 40) °C. After a week, these solutions were measured, following the procedure mentioned above. The accuracy of solubility data can then be confirmed if the solubility data are the same.

The compositions of the liquid phase were determined according to the following method using ICP-OES. A 1 mL of solution, taken using a sampling gun, was sampled and placed into volumetric flask, followed by dilution with deionized water for further analysis. The equilibrium solid-phase was analyzed using an X-ray diffraction diffractometer. The

Table 1. Solubility Data for the Na₂O–V₂O₅–H₂O System

sample no.	composition of liquid phase (g/L)			
	T = 40 °C		T = 80 °C	
	Na ₂ O	V ₂ O ₅	Na ₂ O	V ₂ O ₅
1				
2	193.22	74.39	217.27	132.8
3	219.59	25.41	275.49	81.25
4	244.63	14.30	310.21	68.45
5	249.62	12.94	349.06	56.39
6	264.24	8.44	369.2	50.52
7	278.4	7.79	387.98	45.81
8	303.53	6.18	424.89	44.52
9	317.08	4.89	468.17	42.84
10	343.09	5.33	483.04	43.21
11	375.95	4.12	494.79	42.39
12	418.09	3.95	514.53	43.11
13	419.10	4.21	523.70	42.44
14	454.73	5.04		
15	489.49	8.47		
16	530.97	14.24		

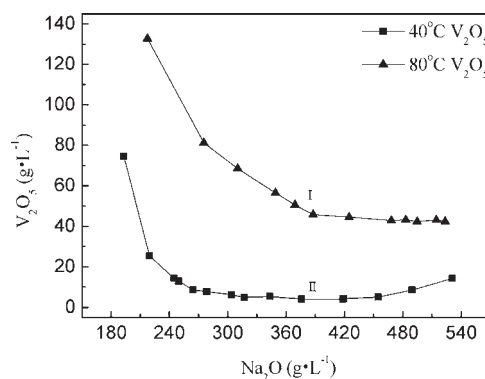


Figure 1. Solubility diagrams of the Na₂O–V₂O₅–H₂O system at (40 and 80) °C: (I) at 40 °C and (II) at 80 °C.

precipitates were sampled according to the following method. First, superstratum solution, used to measure the solution density, was transferred into another clean polyethylene bottle. Then, a small portion of the precipitates was transferred into a clean watch-glass. Then, the solid phase, washed by anhydrous alcohol and dried by air-dry oven, was analyzed by XRD. The superstratum solution was transferred into measuring cylinder of 200 cm³ volume. Then, the solution density was measured by the densimeter, which was calibrated in pure water at (40 and 80) °C.

RESULTS AND DISCUSSION

Na₂O–V₂O₅–H₂O System. The equilibrium data for the Na₂O–V₂O₅–H₂O system are presented in Table 1. Figure 1 shows the solubility diagram of this system. As can be seen in Figure 1, in the low-alkali region (that is the region where the Na₂O concentration < 240 g/L), there is an obvious decrease in the solubility of V₂O₅ with the increase of the Na₂O concentration. So it is possible to separate Na₃VO₄ in this region using

Table 2. Solubility Data of the Na₂O–V₂O₅–CaO–H₂O System at 40 °C

sample no.	ρ	composition of alkaline solution (g·L ⁻¹)			equilibrium crystalline phases
	g·cm ⁻³	Na ₂ O	V ₂ O ₅	CaO	
1	1.051	37.52	0.04	0.056	Ca ₁₀ V ₆ O ₂₅ (A)
2	1.085	67.69	0.20	0.033	Ca ₁₀ V ₆ O ₂₅ (A)
3	1.145	113.08	0.73	0.039	Ca ₁₀ V ₆ O ₂₅ (A)
4	1.170	132.92	5.37	0.042	Ca(OH) ₂ (B) + Ca ₇ V ₄ O ₁₇ (C)
5	1.201	148.70	5.81	0.055	Ca(OH) ₂ (B) + Ca ₇ V ₄ O ₁₇ (C)
6	1.252	173.50	5.29	0.076	Ca(OH) ₂ (B) + Ca ₇ V ₄ O ₁₇ (C)
7	1.318	201.30	5.25	0.114	Ca(OH) ₂ (B) + Ca ₇ V ₄ O ₁₇ (C)
8	1.331	244.96	4.90	0.159	Ca(OH) ₂ (B) + Ca ₇ V ₄ O ₁₇ (C)
9	1.355	295.98	4.91	0.235	Ca(OH) ₂ (B) + Ca ₇ V ₄ O ₁₇ (C)
10	1.382	338.78	4.99	0.295	Ca(OH) ₂ (B) + Ca ₇ V ₄ O ₁₇ (C)
11	1.414	380.69	5.55	0.325	Ca(OH) ₂ (B) + Ca ₇ V ₄ O ₁₇ (C)
12	1.443	414.52	5.82	0.333	Ca(OH) ₂ (B) + Ca ₇ V ₄ O ₁₇ (C)
13	1.462	442.06	6.70	0.341	Ca(OH) ₂ (B) + Ca ₇ V ₄ O ₁₇ (C)
14	1.486	474.03	7.46	0.341	Ca(OH) ₂ (B) + Ca ₇ V ₄ O ₁₇ (C)
15	1.503	527.64	9.18	0.341	Ca(OH) ₂ (B) + Ca ₇ V ₄ O ₁₇ (C)

Table 3. Solubility Data of the Na₂O–V₂O₅–CaO–H₂O System at 80 °C

sample no.	ρ	composition of alkaline solution (g·L ⁻¹)			equilibrium crystalline phases
	g·cm ⁻³	Na ₂ O	V ₂ O ₅	CaO	
1	1.035	38.05	0.06	0.044	Ca ₁₀ V ₆ O ₂₅ (A)
2	1.052	54.38	0.12	0.042	Ca ₁₀ V ₆ O ₂₅ (A)
3	1.075	73.83	0.70	0.037	Ca ₁₀ V ₆ O ₂₅ (A)
4	1.115	97.27	1.58	0.040	Ca(OH) ₂ (B) + Ca ₁₀ V ₆ O ₂₅ (A)
5	1.145	123.16	4.30	0.042	Ca(OH) ₂ (B) + Ca ₁₀ V ₆ O ₂₅ (A)
6	1.173	155.03	11.03	0.058	Ca(OH) ₂ (B) + Ca ₇ V ₄ O ₁₇ (C)
7	1.181	171.57	19.89	0.064	Ca(OH) ₂ (B) + Ca ₇ V ₄ O ₁₇ (C)
8	1.201	193.58	33.69	0.088	Ca(OH) ₂ (B) + Ca ₇ V ₄ O ₁₇ (C)
9	1.289	229.40	37.11	0.117	Ca(OH) ₂ (B) + Ca ₇ V ₄ O ₁₇ (C)
10	1.301	272.80	38.57	0.178	Ca(OH) ₂ (B) + Ca ₇ V ₄ O ₁₇ (C)
11	1.323	313.50	40.61	0.186	Ca(OH) ₂ (B) + Ca ₇ V ₄ O ₁₇ (C)
12	1.344	340.13	41.16	0.189	Ca(OH) ₂ (B) + Ca ₇ V ₄ O ₁₇ (C)
13	1.363	375.44	40.84	0.197	Ca(OH) ₂ (B) + Ca ₇ V ₄ O ₁₇ (C)
14	1.384	402.31	41.33	0.196	Ca(OH) ₂ (B) + Ca ₇ V ₄ O ₁₇ (C)
15	1.409	433.49	42.21	0.196	Ca(OH) ₂ (B) + Ca ₇ V ₄ O ₁₇ (C)
16	1.421	458.12	42.57	0.197	Ca(OH) ₂ (B) + Ca ₇ V ₄ O ₁₇ (C)
17	1.450	480.23	42.43	0.197	Ca(OH) ₂ (B) + Ca ₇ V ₄ O ₁₇ (C)
18	1.467	505.34	42.63	0.205	Ca(OH) ₂ (B) + Ca ₇ V ₄ O ₁₇ (C)
19	1.482	540.09	43.02	0.204	Ca(OH) ₂ (B) + Ca ₇ V ₄ O ₁₇ (C)

evaporative crystallization. However, when the Na₂O concentration is above 240 g/L, the concentration of V₂O₅ does not show any more significant change with an increase of Na₂O concentration. On the other hand, there is an obvious difference in the solubility of V₂O₅ with temperature in the whole Na₂O concentration range. Thus, cooling crystallization is an excellent method of extracting Na₃VO from NaOH solution. However, which method is better depends on the specific process.⁵

Na₂O–V₂O₅–CaO–H₂O System. The equilibrium composition data of the Na₂O–V₂O₅–CaO–H₂O system at (40 and 80) °C were summarized in Tables 2 and 3, and the

corresponding solubility curves were shown in Figure 2. The equilibrium solid phases were examined to be Ca₁₀V₆O₂₅, Ca(OH)₂, and Ca₇V₄O₁₇ in the tables, represented as A, B, and C, respectively. From Table 2 and Figure 2, the solubility of V₂O₅ increased from (0.04 to 9.18) g·L⁻¹ as the Na₂O concentration increased from (37 to 527) g·L⁻¹, and the solubility of CaO increased from (0.056 to 0.341) g·L⁻¹ as the Na₂O concentration increased at 40 °C. It is worth noting that the solubility of V₂O₅ increased significantly at relative low alkalinity (the Na₂O concentration from (37 to 140) g·L⁻¹). However, the solubility does not show any obvious change with

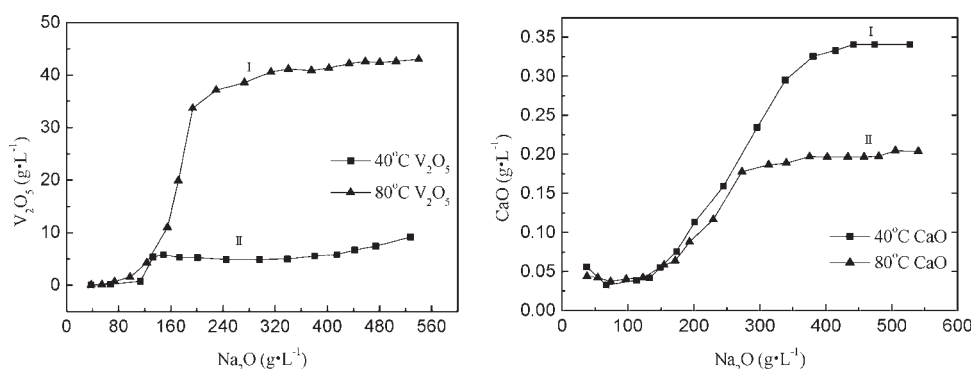


Figure 2. Solubility diagrams of the $\text{Na}_2\text{O}-\text{V}_2\text{O}_5-\text{CaO}-\text{H}_2\text{O}$ system at (40 and 80) °C: (I) at 80 °C and (II) at 40 °C.

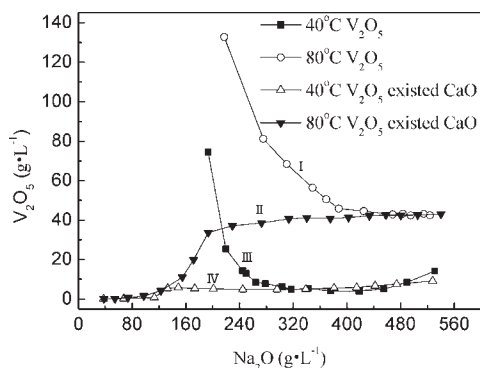


Figure 3. Solubility diagrams of the $\text{Na}_2\text{O}-\text{V}_2\text{O}_5-\text{H}_2\text{O}$ and $\text{Na}_2\text{O}-\text{V}_2\text{O}_5-\text{CaO}-\text{H}_2\text{O}$ systems at (40 and 80) °C: (I) V_2O_5 at 80 °C, (II) V_2O_5 at 80 °C existed CaO, (III) V_2O_5 at 40 °C, and (IV) V_2O_5 at 40 °C existed CaO.

an increase of Na_2O concentration when the Na_2O concentration is above $150 \text{ g}\cdot\text{L}^{-1}$. On the other hand, the time taken for liquid–solid separation was extended with the increase of Na_2O concentration, which was due to the increase of solution density and consequent strengthened buoyancy force with Na_2O concentration.

There is an obvious difference in the solubilities of V_2O_5 and CaO with temperature. From Table 3 and Figure 2, the solubility of V_2O_5 increased from $(0.06 \text{ to } 43.02) \text{ g}\cdot\text{L}^{-1}$ with the Na_2O concentration increasing from $(38 \text{ to } 540) \text{ g}\cdot\text{L}^{-1}$, and the solubility of CaO increased from $(0.044 \text{ to } 0.204) \text{ g}\cdot\text{L}^{-1}$ with the Na_2O concentration increasing at 80 °C. The solubility of V_2O_5 decreased obviously with the decline of temperature at high alkali range. In contrast, the solubility of CaO increased obviously at high alkali range. However, the dissolution phenomenon of V_2O_5 at (40 and 80)°C was similar as suggested by the significant increase of solubility at relative low alkalinity (the Na_2O concentration from $(37 \text{ to } 200) \text{ g}\cdot\text{L}^{-1}$) and slight increase when the Na_2O concentration is above $245 \text{ g}\cdot\text{L}^{-1}$.

$\text{Na}_2\text{O}-\text{V}_2\text{O}_5-\text{H}_2\text{O}$ and $\text{Na}_2\text{O}-\text{V}_2\text{O}_5-\text{CaO}-\text{H}_2\text{O}$ Systems. The V_2O_5 solubility curves of the ternary system ($\text{Na}_2\text{O}-\text{V}_2\text{O}_5-\text{H}_2\text{O}$ system) and quaternary system ($\text{Na}_2\text{O}-\text{V}_2\text{O}_5-\text{CaO}-\text{H}_2\text{O}$) are shown in Figure 3. When CaO was added into the ternary NaOH solution, there is a significant decrease of V_2O_5 concentration (below $280 \text{ g}\cdot\text{L}^{-1}$ Na_2O at 40 °C and below $400 \text{ g}\cdot\text{L}^{-1}$ Na_2O at 80 °C). However, the solubility of V_2O_5 is similar in both the ternary and quaternary systems when the

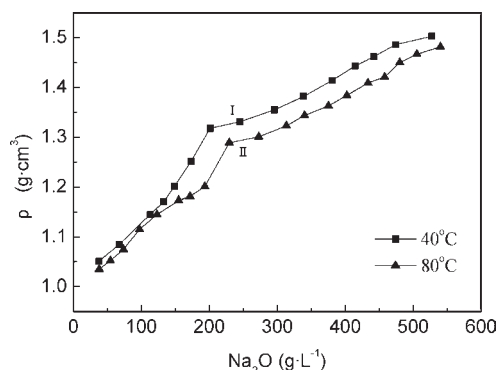


Figure 4. Density data of equilibrium solution at (40 and 80) °C: (I) at 40 °C and (II) at 80 °C. Equilibrium crystalline phases analysis.

Na_2O concentration is above $300 \text{ g}\cdot\text{L}^{-1}$ at 40 °C and the Na_2O concentration is above $440 \text{ g}\cdot\text{L}^{-1}$ at 80 °C.

The density of the equilibrium system, obtained from the NaOH solution containing V_2O_5 and CaO at (40 and 80) °C, is shown in Figure 4. The solution density increased significantly when the Na_2O concentration was below $230 \text{ g}\cdot\text{L}^{-1}$ at (40 and 80) °C. The increase of Na_2O and V_2O_5 concentration is mainly contributed to the increased of solution density in this Na_2O concentration range. However, the solution density increased gently when Na_2O concentration above $230 \text{ g}\cdot\text{L}^{-1}$ at (40 and 80) °C. The increase of Na_2O concentration contributed mainly to the increase of solution density in this Na_2O concentration range. And, the solution density at 40 °C is higher than that of 80 °C.

Figure 5 shows the powder XRD patterns of the precipitate phase obtained at different Na_2O concentration at 80 °C. Three primary XRD patterns are presented as phases of $\text{Ca}_{10}\text{V}_6\text{O}_{25}$, $\text{Ca}(\text{OH})_2 + \text{Ca}_{10}\text{V}_6\text{O}_{25}$, and $\text{Ca}(\text{OH})_2 + \text{Ca}_7\text{V}_4\text{O}_{17}$. However, $\text{Ca}_{10}\text{V}_6\text{O}_{25}$ and $\text{Ca}_7\text{V}_4\text{O}_{17}$ phases carry some similar XRD patterns, and in the analysis, only major peaks were matched to identify $\text{Ca}_{10}\text{V}_6\text{O}_{25}$ or $\text{Ca}_7\text{V}_4\text{O}_{17}$ phases. Thus, the phases of precipitating solids were determined by the optimal matched X-ray diffraction peaks. The precipitate phase obtained at 40 °C from XRD pattern analysis was similar to that found at 80 °C. The only difference was that the precipitate, obtained from 40 °C, did not show $\text{Ca}(\text{OH})_2 + \text{Ca}_{10}\text{V}_6\text{O}_{25}$ phase.

Precipitate Reaction Analysis. From the solubility diagrams and the powder XRD patterns of the precipitate phase, it is known that the major reactions are diverse at different concentrations of Na_2O solution. Reaction 2 dominates when the Na_2O

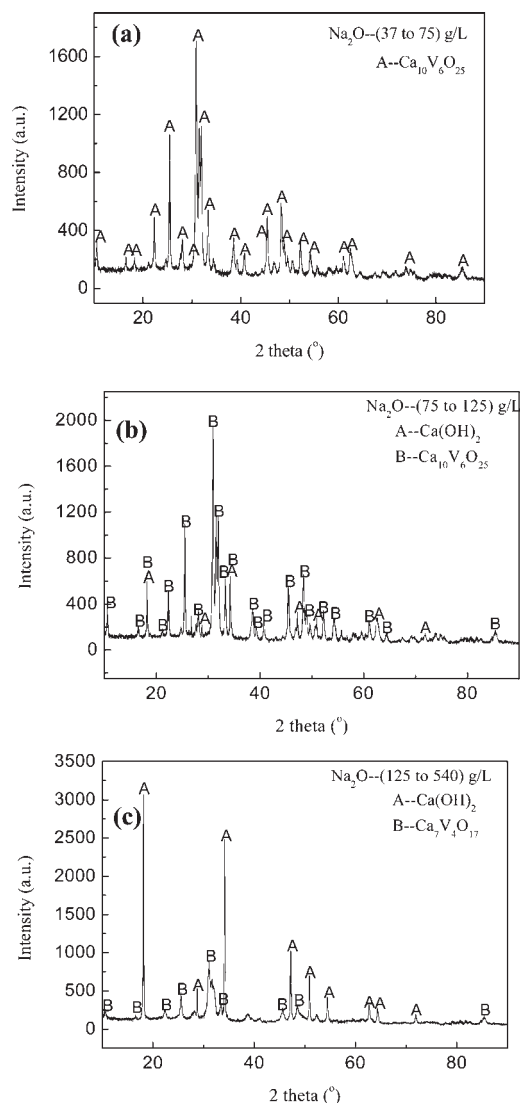
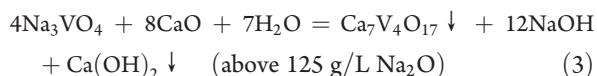
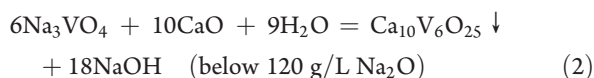


Figure 5. XRD patterns for the precipitate phase obtained from the Na_2O solution at $(37 \text{ to } 75) \text{ g}\cdot\text{L}^{-1}$ (a), $(75 \text{ to } 125) \text{ g}\cdot\text{L}^{-1}$ (b), and $(125 \text{ to } 540) \text{ g}\cdot\text{L}^{-1}$ (c), at 80°C .

concentration is below $120 \text{ g}\cdot\text{L}^{-1}$, and reaction 3 dominates when the Na_2O concentration region above $125 \text{ g}\cdot\text{L}^{-1}$. The reactions are presented as follows:



CONCLUSIONS

Solubility data for the $\text{Na}_2\text{O}-\text{V}_2\text{O}_5-\text{CaO}-\text{H}_2\text{O}$ system and sub system at $(40 \text{ and } 80)^\circ\text{C}$ were investigated in this study. From the data, a method of producing calcium vanadate from Na_3VO_4 and leaching calcium vanadate from vanadium slag by calcination with calcium or other materials containing calcium is proposed. Relative low NaOH concentration ($< 190 \text{ g}\cdot\text{L}^{-1}$)

could be elected for the precipitation of calcium vanadium due to the low solubility of vanadium compounds at this concentration range. Thus, a NaOH concentration of larger than $200 \text{ g}\cdot\text{L}^{-1}$ could be chosen for the leaching of calcium vanadate due to the large vanadium compound solubility, and enhanced temperature is beneficial for the leaching reaction.

AUTHOR INFORMATION

Corresponding Author

*E-mail: shnwang@home.ipe.ac.cn. Phone: +86-10-82544856. Fax: +86-10-82544856.

Funding Sources

The authors gratefully acknowledge the financial support from the National Natural Science Foundation of China under Grant Nos. 51090382 and 50874099 and the National High Technology Research and Development Program of China (863 program) under Grant No. 2009AA064003.

REFERENCES

- (1) Subba Reddy, Ch. V.; Wei, J.; Quan-Yao, Z.; Zhi-Rong, D.; Wen, C.; Mho, S.-i.; Kalluru, R. R. Cathodic performance of $(\text{V}_2\text{O}_5 + \text{PEG})$ nanobelts for Li ion rechargeable battery. *J. Power Sources* **2007**, *166*, 244–249.
- (2) Grégoire, G.; Soudan, P.; Farcy, J.; Pereira-ramos, J.-P.; Badot, J.-C.; Baffier, N. Electrochemical lithium insertion in the hexagonal cesium vanadium bronze $\text{Cs}_{0.35}\text{V}_2\text{O}_5$. *J. Power Sources* **1999**, *81–82*, 612–615.
- (3) Subba Reddy, Ch. V.; Yeo, I.-H.; Mho, S.-i. Synthesis of sodium vanadate nanosized materials for electrochemical applications. *J. Phys. Chem. Solids* **2008**, *69*, 1261–1264.
- (4) Zhao, T. C. *Non-ferrous Extractive Metallurgy Handbook*; Metallurgy Industry Press: Beijing, 2002.
- (5) Wang, S. N.; Song, Z. W.; Zhang, Y.; Du, H.; Zhang, Y. Solubility data for the $\text{NaOH}-\text{NaNO}_3-\text{Na}_3\text{VO}_4-\text{Na}_2\text{CrO}_4-\text{H}_2\text{O}$ system at $(40 \text{ and } 80)^\circ\text{C}$. *J. Chem. Eng. Data* **2010**, *55*, 4607–4610.
- (6) Moskalyk, R. R.; Alfantazi, A. M. Processing of vanadium: a review. *Miner. Eng.* **2003**, *16*, 793–805.
- (7) Huo, Q.; Margolese, D.; Ciesla, U. A simplified kinetic model for an autopoietic synthesis of micelles. *Chem. Mater.* **1994**, *6*, 1176–1178.
- (8) Chang, J. Y.; Jung, D. Y. Hydrothermal Synthesis of Mesoporous Vanadium Oxide and Application of UV-Ozone Treatment. *Bull. Korean Chem. Soc.* **2003**, *24* (5), 613–616.
- (9) Skyllas-Kazacos, M.; Robbins, R. G. All vanadium redox battery. U.S. Patent No. 849,094, 1986.
- (10) Zhang, S. H.; Yin, C. X.; Xing, D. B.; Yang, D. L.; Jian, X. G. Preparation of chloromethylated/quaternized poly (phthalazinone ether ketone) anion exchange membrane materials for vanadium redox flow battery applications. *J. Membr. Sci.* **2010**, *243*–249.
- (11) Rydh, C. J. Environmental assessment of vanadium redox and lead-acid batteries for stationary energy storage. *J. Power Sources* **1999**, *80*, 21–29.
- (12) Rajab, V. R. Vanadium market in the world. *Steel World* **2007**, 19–22.
- (13) Wang, H. S. Extraction of vanadium from stone coal by roasting in the presence of sodium salts; 1994, *14* (2), 49–52.
- (14) Wang, J. C. Effect of Calcium on Leaching of Vanadium from Vanadium slag. *Sichuan Nonferrous Met.* **2004**, *4*, 27–29.
- (15) Bin, Z. Y. Study on Extraction of V_2O_5 from Vanadium Ore By Roasting and Acid Leaching Process. *Iron Steel Vanadium Titanium* **2006**, *27* (1), 21–26.
- (16) Zheng, S. L.; Du, H.; Wang, S. N.; Wang, X. H.; Zhang, Y. One decomposition method of vanadium slag is oxidized by NaOH solution. Chinese patent, No. 201010034089.5.